Temperature measured close to the interface of an evaporating liquid

G. Fang* and C. A. Ward†

Department of Mechanical and Industrial Engineering, University of Toronto, 5 King's College Road, Toronto, Ontario, Canada M5S 3G8

(Received 18 February 1998)

Recent measurements of the temperature profile across the interface of an evaporating liquid are in strong disagreement with the predictions from classical kinetic theory or nonequilibrium thermodynamics. However, these previous measurements in the vapor were made within a minimum of 27 mean free paths of the interface. Since classical kinetic theory indicates that sharp changes in the temperature can occur near the interface of an evaporating liquid, a series of experiments were performed to determine if the disagreement could be resolved by measurements of the temperature closer to the interface. The measurements reported herein were performed as close as one mean free path of the interface of an evaporating liquid. The results indicate that it is the higher-energy molecules that escape the liquid during evaporation. Their temperature is greater than that in the liquid phase at the interface and as a result there is a discontinuity in temperature across the interface that is much larger in magnitude (up to 7.8 °C in our experiments) and in the opposite direction to that predicted by classical kinetic theory or nonequilibrium thermodynamics. The measurements reported herein support the previous ones. [S1063-651X(98)11312-0]

PACS number(s): 68.10.Jy

I. INTRODUCTION

Recent analytical studies based on a variety of classical kinetic theory models have indicated that the Hertz-Knudsen relation for predicting the rate of evaporation could be in error by as much as 70% [1–3]. However, these analytical procedures also indicated a surprising result for the ''two-plate experiment'' in which evaporation occurs at one liquid film and condensation at the other. For a monatomic substance evaporating and condensing in this circumstance, it was predicted that if the ratio of the latent heat to the product of the gas constant and the temperature (i.e., h_{fg}/RT) was greater than approximately 4.5, the temperature profile in the vapor would be in the opposite direction to that applied to the plates [2]. Since such temperature profiles seem nonphysical, they have been referred to as ''anomalous'' [3] and ''inverted'' [4,5]. If water is the substance considered, then one finds that an inverted profile would be expected if the temperature at which the evaporation occurred were less than approximately 65 °C.

A necessary condition for the inverted temperature profile to exist is that the temperature on the vapor side of the evaporating liquid-vapor interface be *less* than that on the liquid side. Two experimental studies have been reported of the temperature near the interface of an evaporating liquid [3,6]. Shankar and Deshpande studied water evaporation under a quasi-steady-state circumstance, but for water were not able to detect a temperature discontinuity at the liquid-vapor interface [3]. Their experiments are difficult to interpret since they were not able to hold the liquid-vapor interface in a steady state. Recently, a method was introduced that allows the temperature to be measured across a liquid-vapor interface during steady-state evaporation [6]. With water evaporating at five different rates, it was found in each case that (i) there is a temperature discontinuity at the interface, (ii) the magnitude of the temperature discontinuity is much larger than expected from either classical kinetic theory [1,2,5] or nonequilibrium thermodynamics [7] predictions, and (iii) the discontinuity is in the *opposite* direction from that predicted by classical kinetic theory or nonequilibrium thermodynamics [1,2,5,7].

In view of the disagreement between theory [1,2,7] and experiments [6], it seems appropriate to seek an explanation. One of the possibilities is that there is a sharp gradient in the temperature within the Knudsen layer where classical kinetic theory suggests such changes could exist [8]. With the thermocouples used in the previous study of steady-state evaporation, it was only possible to measure within approximately 0.5 mm of the interface. This corresponds to measuring the temperature within approximately 27 mean free paths of the interface. In order to examine the temperature near the interface of an evaporating liquid, we have redesigned the experimental apparatus to allow the temperature in the vapor to be measured within approximately one mean free path and to study higher rates of evaporation.

Also, in the previous study there was the possibility that the temperature gradient affected the temperature measurement [9,10]. The temperature in the vapor at the interface was lower than it was at any other point in the vapor and the thermocouple was oriented parallel to the temperature gradient. Thus there was the possibility that energy would be conducted down the thermocouple wire and have caused the thermocouple to read a higher temperature in the vapor near the interface than actually existed there. If such an effect were sufficiently large, it could eliminate the discrepancy between the theory and the measurements. This effect is examined by using thermocouples of different sizes in the same evaporation experiment.

*Present address: Trojan Technologies, Inc., 3020 Gore Road, London, Ontario, Canada N5V 4T7.

†Author to whom correspondence should be addressed. FAX: 416-978-7322. Electronic address: ward@mie.utoronto.ca

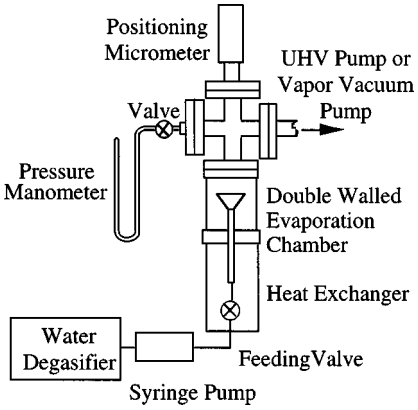

FIG. 1. Simplified schematic of the experimental apparatus.

II. EXPERIMENTAL APPARATUS, METHODS, AND PROCEDURES

A. Evaporation chamber

The (modified [6]) evaporation apparatus is shown schematically in Fig. 1 and the evaporation chamber in Fig. 2. The chamber is double walled and the space between the walls was evacuated with a mechanical vacuum pump (not shown, Pfeiffer, DUO 1.5 A, Germany). A glass funnel was installed on the center line of the chamber. During the experiments, the water was supplied at the bottom of the glass funnel by a computer controlled, syringe pump (Cole-Palmer 74900-10). The liquid interface was located at the top of the funnel where it was exposed to the vapor. The interface height could be observed by a cathetometer and measured with an accuracy of ± 10 μm. As indicated in Fig. 3, an image of the liquid-vapor interface could be recorded through the clear (acrylic) walls of the evaporation chamber by a charge coupled device (CCD) camera.

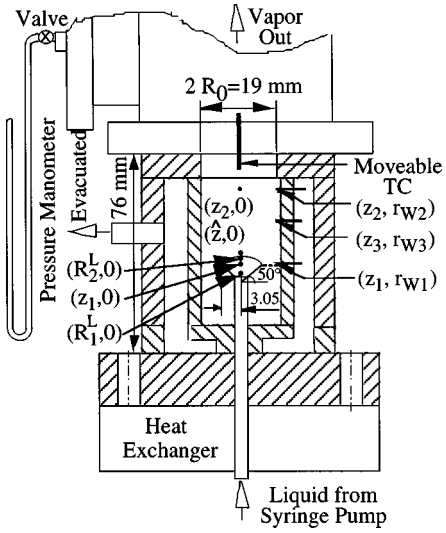

FIG. 2. Schematic of the evaporation chamber and the positions where measurements were made with thermocouples (TC) of the temperature: $T_{M1}(z_2,0)$, $T_{M2}(z_2,r_{w2})$, $T_{M3}(z_1,r_{w1})$, $T_{M4}(z_3,r_{w3})$, and $T_{M5}(\hat{z},0)$ in the vapor. In addition, the temperature was measured on the center line with a movable thermocouple from $(\hat{z},0)$ to $(z_2,0)$ in the vapor and from $(R_1^L,0)$ to $(R_2^L,0)$ in the liquid.

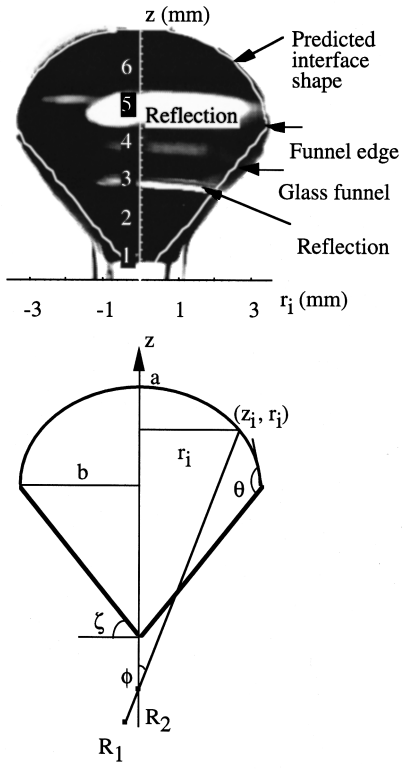

FIG. 3. Image of the liquid-vapor interface captured through the double walls of the evaporation chamber by a CCD camera and the predicted interface shape when the liquid evaporation rate was 160 μl/h. Its height is denoted as a. The lines were drawn from the center of the coordinate system and are tangential to the glass surface at its outer edge of the cone. The angle ζ was 50° and the value of b was 3.05 mm.

Three thermocouples were located just inside the inner chamber wall using a vacuum epoxy (Torr Seal, Varian). One thermocouple was installed on the wall of the inner chamber at the same height as that of the glass funnel edge. In the experiments, the liquid phase filled the funnel up to the funnel edge. Thus the measurement of the temperature on the wall of the inner chamber spanned the height of the vapor phase.

The pressure in this chamber was controlled by opening or closing a vacuum valve in a line that leads to a mechanical vacuum pump (Welch DuoSeal 1400). This allowed the pressure to which the liquid was exposed, and therefore the evaporation rate of the liquid, to be changed. By adjusting the flow rate of the liquid entering the chamber and the pressure in the vapor, the position of the liquid interface could be maintained unchanged during an experiment.

B. Temperature measurement

Since the temperature change close to the interface is severe, a small thermocouple is required to measure the temperature in the vapor within a few mean free paths of the interface. For this purpose, a junction was formed between chromel and alumel wires that were 25.4 μm (0.001 in.) in diameter using a mini hydrogen-oxygen torch (0.152-mm-diam orifice, Smith Equipment). The resulting weld bead was examined under a microscope and found to be approximately twice the size of the wire. The alumel and chromel

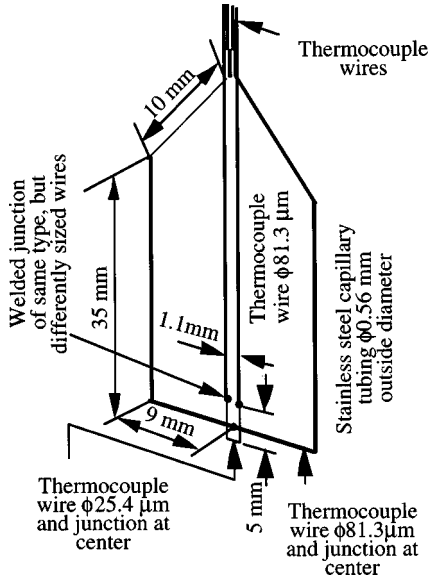

FIG. 4. Configuration of movable thermocouples in the evaporation chamber. Two differently sized thermocouples, 25.4 and 81.3 μm in diameter, were used.

wires were then fashioned into a U shape and each end welded to a thicker (80.3-μm-diam) alumel or a chromel wire, as indicated in Fig. 4. The thick wires were attached to a Teflon bar for support. The ratio of the length of a horizontal portion of the thermocouple to the diameter of the thermocouple junction was approximately 21.6. When the length of the horizontal section is approximately 20 times the diameter of the junction, the conduction along the wire is expected to be negligible [9,10].

For comparison a second thermocouple of the same type that had a larger diameter (81.3 μm) was also constructed and mounted relative to the smaller thermocouple as indicated in Fig. 4. The larger thermocouple was also fashioned into a U shape and had a horizontal section that was 110 times its junction diameter. The device shown in Fig. 4 was then mounted on a positioning micrometer (see Fig. 1) that allowed the two thermocouples to be moved 20 mm vertically on the center line of the evaporation chamber. This permitted the large thermocouple to be used to measure the temperature within 0.2 mm of the interface, but the smaller thermocouple could be used to measure the temperature within 0.03 mm of the interface. Away from the interface, the differently sized thermocouples could be used to measure the temperature at the same position. The position of the large thermocouple at the time of a measurement was established with the cathetometer; however, the smaller thermocouple was too small to be seen with the cathetometer when it was in the double-walled evaporation chamber. Its position was determined with the positioning micrometer (with accuracy ± 10 μm).

C. Pressure measurement

The inner cylinder of the evaporation chamber was connected to an ultrahigh vacuum (UHV) pumping system using O-ring seals (see Fig. 1). The pressure was measured with vacuum gauges (Balzers cold cathode IKR 020 and Pirani TPR 017/018, not shown). These allowed the pressure of this chamber to be measured from atmospheric down to 10^{-8} Pa. However, these measurements were approximately 400 mm away from the liquid-vapor interface.

In order to measure the pressure closer to the liquid-vapor interface, a closed-end, U-shaped absolute mercury manometer was connected to the apparatus as indicated in Figs. 1 and 2. The accuracy of the mercury column reading was ± 13.3 Pa. A vacuum valve was installed between the manometer and the system to isolate the manometer when the manometer was not in use. The position of the mercury level was set at approximately the same level as the interface. During the evaporation experiment, both the Pirani gauge and the manometer were used.

After the experiments were conducted, with no liquid in the evaporation chamber, the manometer was calibrated by partially opening the value to the UHV system. This allowed the pressure to be reduced to approximately 0.93 Pa, as read by the Piranni gauge. The vapor pressure of Hg at room temperature is 0.13 Pa. Thus the Hg evaporation should be negligible. After the calibration, the absolute pressure in our experiments indicated by the Hg manometer ranged from 195 to 596 Pa.

D. Liquid inlet temperature control

In order to control the temperature of the liquid at the inlet to the evaporation chamber, the liquid passed through a heat exchanger that was constructed from a water bath circulator (HAAKE F3, Germany), a fan (Major Tubeaxial AC fan, Model MR 2B3, Electronic), and a liquid-air heat exchanger (modified from a vehicle radiator). A 25-cm-long segment of the tube ($\frac{1}{16}$ in. in diameter) carrying the liquid from the syringe pump to the funnel was passed through the heat exchanger. It was found that this system could control the temperature of the liquid entering the funnel to within ± 0.8 °C over a range of 10 °C–40 °C.

E. Mass spectrometer measurement

A sample of gas from the inner cylinder of the evaporation chamber could be drawn through a leak valve into a quadrupole mass spectrometer (Dataquad DXM, Spectramass Ltd. or OMG 064, Balzer) that was attached to the ultrahigh vacuum pumping system. Gas samples from the evaporation chamber could be taken during an experiment without noticeably changing the conditions in the evaporation chamber. The residual gases in the system before the experiment were primarily H_2O and N_2. During the experiment, H_2O was the only substance above the background.

F. Experimental procedure

Before an experiment, the evaporation chamber was evacuated to a pressure of 10^{-3} Pa and held at this condition for over 10 h in order to minimize the gaseous impurities [11]. The water to be used in an experiment was distilled, de-ionized, and filtered (Nanopure, Barnstead). Its resistance was $15.0M\ \Omega$ cm and its surface tension was 71.6 ± 1.2 mN/m at 25.5 °C. Before a water sample was placed in the syringe, it was degassed. A 2-ml water sample was then transferred from the degassing vessel directly into the syringe of the injection pump.

After isolating the evaporation chamber from the ultrahigh vacuum system, dry N_2 gas was introduced into the evaporation chamber until the pressure was approximately 10^4 Pa. Then a low flow rate was set on the syringe pump and the water was allowed to advance into the evaporation chamber until the interface was visible above the funnel edge. The syringe pump was then stopped and the nitrogen pressure was increased to 0.3 MPa and held at this condition for approximately 1 h. It was found that if the pressurization phase were undertaken, the pressure in the vapor could subsequently be reduced to near the saturation vapor pressure without bubble nucleation occurring in the liquid phase.

Once the pressurization phase had been completed, the pressure in the vaporization chamber was lowered with the vacuum pump and the liquid flow rate into the evaporation chamber increased. The temperature of the heat exchanger was set so that the liquid entering the evaporation chamber was at a predetermined value. The system was then brought to a steady state with the liquid evaporating by adjusting the pressure in the vapor and the liquid injection rate.

The criterion for determining if a steady state had been reached was to observe the liquid-vapor interface for a period of at least 2 h; if no change in the height of the interface was measurable with the cathetometer nor was there any measurable change in the pressure of the vapor by either the manometer or the Pirani gauge, then the system was assumed to be operating under steady-state conditions. If changes were observed in either the interface height or the pressure, adjustments were made and the 2-h observation period repeated. During this period of evaporation, only pure liquid was entering at the bottom of the tube leading to the funnel and the liquid evaporating at the top of the funnel would have contained gas dissolved in the liquid during the pressurization phase. Thus, as the evaporation proceeded, the evaporating liquid was progressively purer.

Once a steady state had apparently been reached, the temperature could be measured in the vapor and in the liquid phase with the movable thermocouples. The position of the thermocouples at the time of a measurement was determined with the cathetometer and the positioning micrometer. To confirm that the system was operating in a steady state, the procedure adopted was to allow the liquid to continue to evaporate for approximately 1 h after the first set of temperatures had been recorded and then to repeat the temperature measurements. If the temperatures recorded in the second set of measurements at each position agreed with the first set to within a fraction of a degree, the assumption of steady state was taken to be valid. If the agreement was not within this tolerance, then the system was allowed to continue operating for another hour before taking another set of temperature measurements. When two sets of measurements agreed to within a fraction of a degree at each point, the system was taken to be operating in a steady state. Also, since the liquid would have been evaporating for at least 3 h when the second set of measurements was made and the liquid would have been purer at this time than when the first set of measurements was made, any remaining dissolved gas was assumed to have only a negligible effect on the steady-state evaporation. The analytical procedure described in Ref. [6] indicates that for the lowest rate of evaporation that we consider herein, the N_2 concentration before the second set of measurements was made would be less than 2% of the saturation value.

III. EXPERIMENTAL RESULTS

Three sets of experiments were performed. In each set, the temperature of the liquid entering the evaporation chamber was set at 15 °C, 26 °C, or 35 °C using the heat exchanger indicated in Figs. 1 and 2. Then the system was

TABLE I. Summary of water evaporation experiments.

Liquid evaporation rate (μl/h)	Pressure in the vapor (Pa)	Mean free path (μm)	Position in MFP's from interface where temperature measured in the vapor	Temperature measured in the vapor (°C)	Depth in the liquid from the interface where temperature measured (mm)	Temperature measured in the liquid T_{NI}^{L} (°C)	Evaporation flux $\overline{j}$ (g m^{-2} s^{-1})
70[a]	596.0	9.1	2.2	3.3±0.1	0.18	−0.2±0.1	0.2799
75[b]	493.3	10.8	3.7	0.9±0.1	0.21	−2.8±0.1	0.2544
85[b]	426.6	12.3	1.6	−0.5±0.1	0.23	−4.7±0.1	0.3049
90[a]	413.3	12.7	1.7	−0.9±0.1	0.19	−5.1±0.0	0.4166
100[b]	310.6	16.7	1.8	−3.6±0.1	0.22	−8.7±0.2	0.3703
100[b]	342.6	14.8	4.7	−2.3±0.1	0.08	−7.6±0.1	0.3480
100[c]	333.3	15.9	1.3	−1.5±0.1	0.23	−7.7±0.0	0.3971
110[a]	269.3	18.7	2.7	−4.2±0.0	0.30	−10.5±0.0	0.4081
110[b]	277.3	18.5	1.6	−4.1±0.2	0.22	−10.2±0.0	0.4347
120[a]	264.0	18.7	1.4	−4.8±0.0	0.13	−11.0±0.2	0.4097
120[c]	269.3	18.9	1.3	−4.0±0.1	0.18	−10.5±0.1	0.4860
130[a]	245.3	19.8	2.0	−5.8±0.1	0.16	−11.8±0.0	0.4166
140[c]	233.3	21.6	1.9	−4.9±0.1	0.22	−12.3±0.1	0.4938
150[c]	213.3	22.5	2.2	−5.9±0.1	0.15	−13.4±0.0	0.5086
160[c]	194.7	25.3	1.2	−6.5±0.5	0.22	−14.5±0.0	0.5386

[a]The liquid temperature entering the evaporation chamber was 26 °C.
[b]The liquid temperature entering the evaporation chamber was 15 °C.
[c]The liquid temperature entering the evaporation chamber was 35 °C.

brought to a steady state with the liquid evaporating at a constant rate. The temperature was recorded on the center line of the evaporation chamber with the differently sized thermocouples and the positioning micrometer. At each experimental condition, the temperature was measured at approximately 1-mm intervals in the bulk vapor phase. Near the interface, it was measured at approximately 0.1-mm intervals. The range over which the temperature was measured was from a depth of approximately 2 mm into the liquid phase to a height of 18 mm above the interface. The shape of the thermocouple probe prevented the temperature from being measured to a greater depth. In the repeated measurement of temperature approximately 1 h apart using the thin thermocouple, it was found that the maximum deviation at one position was 0.9 °C and the minimum was 0.1 °C.

The conditions existing in the evaporation chamber in each experiment are listed in Table I. For the case of water entering the evaporation chamber at 35 °C, with a pressure in the vapor of 194.7 Pa and an evaporation rate of 160 μl of liquid per hour, the temperature profile measured in the two phases is shown in Fig. 5. In Figs. 5(a) and 5(b) the values obtained in the repeated measurements by the differently sized thermocouples are indicated and those close to the interface are shown in more detail in Fig. 5(b). Also in this figure the position of the interface is indicated by a vertical solid line and the calculated position of one mean free path from the interface in the vapor is also shown by a vertical line.

A summary of all of our experimental results is given in Table I. As may be seen there the evaporation rate was varied from 70 to 160 μl of liquid per hour and the mean free path varied from 9 to 25 μm. In the liquid phase, the temperature was measured to within less than 0.25 mm of the interface and in the vapor the position where the temperature was measured was 1 to 5 mean free paths from the interface. In all cases the temperature in the vapor was *larger* than that in the liquid. The maximum difference occurred in the experiment with the highest evaporation rate and was 8 °C.

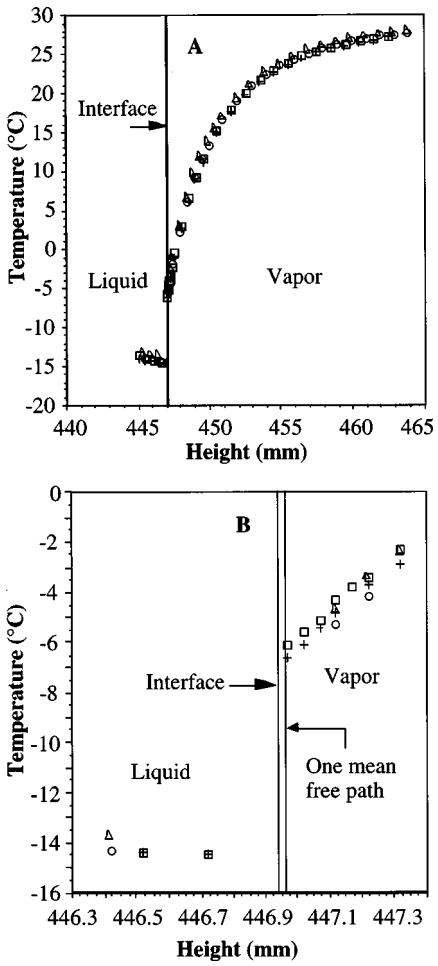

FIG. 5. (a) Temperatures measured repeatedly using differently sized thermocouples in the experiment with a 160-μl/h liquid evaporation rate. (b) Temperatures measured close to the liquid-vapor interface in the same experiment. The open squares, crosses, open triangles, and open circles indicate the temperature measurements. The open squares are the first measurement with the thin thermocouple and the crosses are the repeated measurement with the thin thermocouple. The open triangles are the first measurement with the large thermocouple and the open circles are the repeated measurement with the large thermocouple. The position of the interface is indicated by a vertical solid line and the position one mean free path away from the interface is also indicated by a vertical line. The abscissa is the height measured with the cathetometer when the origin is at 440.24 mm.

IV. EXPRESSION FOR TEMPERATURE PROFILES IN VAPOR AND LIQUID PHASES

Since the temperature in the vapor has been measured from approximately 1 to 640 mean free paths from the interface, the measurements near the interface can be used to examine the predictions that have been made regarding the temperature profile there.

A. Temperature profile in the vapor

For the experiments that we report, the maximum Mach number is 2.3×10^{-4}. This allows the axisymmetric, steady-state continuum energy equation in cylindrical coordinates (z,r) to be simplified [6]. If the temperature nearest the interface in the liquid phase is denoted as T_{NI}^{L} and the nondimensional temperature $\overline{T}$ is defined as

$$\overline{T}=\frac{T(z,r)-T(z_2,0)}{T_{NI}^{L}} \tag{1}$$

then one finds that the simplified energy equation may be written

$$\mathrm{Pe}\,\frac{\partial}{\partial\overline{z}}\overline{T}=\frac{1}{\overline{r}}\frac{\partial}{\partial\overline{r}}\left(\overline{r}\,\frac{\partial}{\partial\overline{r}}\overline{T}\right)+\frac{\partial^2}{\partial\overline{z}^2}\,\overline{T}, \tag{2}$$

where the position coordinates have been nondimensionalized with the radius of the evaporation chamber R_0 (see Fig. 2), and the Péclet number Pe is given by

$$\mathrm{Pe}=\frac{P^V u R_0 C_P^V}{\kappa^V},$$

where P^V is the density of the vapor, u is the fluid speed which we approximate as uniform, and C_P^V and κ^V are the constant pressure-specific heat and the thermal conductivity of the vapor.

If the temperatures measured at the positions $(z_2,0)$, (z_2,r_{w2}), and (z_1,r_{w1}) indicated in Fig. 2 are denoted as T_{M1}, T_{M2}, and T_{M3} and $\overline{T}_0$ is a value of the nondimensional temperature that is assigned to the position $(z_1,0)$, then following the procedure of Ref. [6], we assume that the temperature at the upper boundary of the vapor may be approximated as

$$\overline{T}(\overline{z}_2,\overline{r})=\overline{T}_{M1}+\overline{r}^2(\overline{T}_{M2}-\overline{T}_{M1}) \tag{3}$$

and at the bottom as

$$\overline{T}(\overline{z}_1,\overline{r})=\overline{T}_0+\overline{r}^2(\overline{T}_{M3}-\overline{T}_0). \tag{4}$$

As the boundary condition on the lateral surface of the vapor we assume

$$\left(\frac{\partial\overline{T}}{\partial\overline{r}}\right)_{\overline{r}=1}=\frac{\mathrm{Nu}}{2}\,\overline{T}(\overline{z},1), \tag{5}$$

where Nu is the Nusselt number ($2R_0h/\kappa^V$; κ^V is the thermal conductivity of the vapor and h is the heat transfer coefficient). The values of Nu and $\overline{T}_0$ will be assigned by the same procedure as that of Ref. [6].

The solution to the energy equation may be written in terms of Bessel functions and after requiring the solution to be bounded on the axis, one finds

$$\overline{T}=\sum_{\lambda=0}^{\infty}(N_\lambda e^{m_1\overline{z}}+M_\lambda e^{m_2\overline{z}})J_0(q_\lambda\overline{r}), \tag{6}$$

where $J_0(q_\lambda\overline{r})$ is the zeroth-order Bessel function of the first kind and

$$m_1=\frac{\mathrm{Pe}-\sqrt{\mathrm{Pe}^2+4q_\lambda^2}}{2},\quad m_2=\frac{\mathrm{Pe}+\sqrt{\mathrm{Pe}^2+4q_\lambda^2}}{2}. \tag{7}$$

After applying the boundary condition given in Eqs. (3)–(5) and taking advantage of the orthogonality properties of the Bessel functions, one finds

$$q_\lambda=-\frac{\mathrm{Nu}}{2}\frac{J_0(q_\lambda)}{J_1(q_\lambda)}, \tag{8}$$

$$N_\lambda=2\frac{e^{-m_2\overline{z}_1}\int_0^1\overline{r}\,\overline{T}(\overline{z}_1,\overline{r})J_0(q_\lambda\overline{r})d\overline{r}-e^{-m_2\overline{z}_2}\int_0^1\overline{r}\,\overline{T}(\overline{z}_2,\overline{r})J_0(q_\lambda\overline{r})d\overline{r}}{[J_1^2(q_\lambda)+J_0^2(q_\lambda)](e^{(m_1-m_2)\overline{z}_1}-e^{(m_1-m_2)\overline{z}_2})}, \tag{9}$$

and

$$M_\lambda=\frac{2e^{-m_2\overline{z}_2}\int_0^1\overline{r}\,\overline{T}(\overline{z}_2,\overline{r})J_0(q_\lambda\overline{r})d\overline{r}}{J_1^2(q_\lambda)+J_0^2(q_\lambda)}-N_\lambda e^{(m_1-m_2)\overline{z}_2}. \tag{10}$$

The values of N_λ and M_λ depend implicitly on the value of Nu and $\overline{T}_0$. To determine the values of N_λ and M_λ, we will use the temperatures measured in the vapor at five positions: $\overline{T}_{M1},\overline{T}_{M2},\ldots,\overline{T}_{M5}$. As indicated in Fig. 2, $\overline{T}_{M4}$ is the temperature measured at (z_3,r_{w3}) and $\overline{T}_{M5}$ is the temperature measured with the movable thermocouple at the position $(\hat{z},0)$. If the nondimensional temperature calculated at each of these positions is denoted as $\overline{T}T_{Cj}$, $j=1,\ldots,5$, then a measure of the error between the calculated temperature and the measured temperature at these points is

$$E=\sum_{j=1}^{5}(\overline{T}_{Cj}-\overline{T}_{Mj})^2. \tag{11}$$

Since the calculated temperature depends on $\overline{T}_0$ and Nu as parameters, the best values to choose for these parameters would be those values that give the minimum error. This requires

$$\left(\frac{\partial E}{\partial\,\mathrm{Nu}}\right)_{\overline{T}_0=\overline{T}_{0B},\mathrm{Nu}=\mathrm{Nu}_B}=0 \tag{12}$$

and

$$\left(\frac{\partial E}{\partial\overline{T}_0}\right)_{\overline{T}_0=\overline{T}_{0B},\mathrm{Nu}=\mathrm{Nu}_B}=0. \tag{13}$$

Using the numerical procedure described in Ref. [6] and the measured values of the temperature to be used as the boundary conditions that are given in Table II, the values of $\overline{T}_0$ and Nu may be determined from Eqs. (12) and (13). The values obtained for each experiment are listed in Table III. Once the values of $\overline{T}_0$ and Nu have been determined, they may be used to calculate the heat flux from the vapor to the liquid-vapor interface $\overline{Q}_V$. If the coordinates of a point on the interface are denoted as r_i,z_i, then they may be expressed as a function of the turning angle ϕ and the heat flux expressed as

$$\overline{Q}_V=\frac{2\pi}{A_I}\int_0^{\theta-\zeta}\frac{r_i[-\kappa^V(\vec{\nabla}T)_{IV}\cdot\vec{n}_I]}{\left[\frac{2}{R_c}+\left(\frac{\rho^Lg}{\gamma^{LV}}\right)\left(a-z_i-\frac{\sin\phi}{r_i}\right)\right]}\,d\phi, \tag{14}$$

TABLE II. Measured temperatures in the vapor that are used as boundary conditions.

Liquid evaporation rate (μl/h)	Position $[z_2$ (mm), 0] and T_{M1} (°C)	Position (z_2, z_{w2}) (mm) and T_{M2} (°C)	Position (z_1, z_{w1}) (mm) and T_{M3} (°C)	Position (z_3, z_{w3}) (mm) and T_{M4} (°C)	Position $[\hat{z}$ (mm), 0] and T_{M5} (°C)
70[a]	(22.4, 0)	(22.41, 8.13)	(15.88, 8.13)	(3.48, 8.13)	(6.40, 0)
	26.1±0.0	26.9±0.0	25.5±0.1	24.3±0.0	4.3±0.1
75[b]	(22.28, 0)	(22.41, 8.13)	(15.88, 8.13)	(3.48, 8.13)	(7.28, 0)
	22.7±0.1	23.6±0.0	21.9±0.1	19.9±0.5	4.9±0.1
85[b]	(22.43, 0)	(22.41, 8.13)	(15.88, 8.13)	(3.48, 8.13)	(6.73, 0)
	23.2±0.1	24.1±0.1	22.5±0.1	20.9±0.1	1.4±0.1
90[a]	(22.33, 0)	(22.41, 8.13)	(15.88, 8.13)	(3.48, 8.13)	(6.63, 0)
	24.5±0.1	25.3±0.1	23.8±0.1	22.5±0.1	1.3±0.1
100[b]	(22.23, 0)	(22.41, 8.13)	(15.88, 8.13)	(3.48, 8.13)	(6.68, 0)
	23.1±0.1	24.1±0.1	22.3±0.1	20.6±0.1	−1.3±0.1
100[b]	(22.25, 0)	(22.41, 8.13)	(15.88, 8.13)	(3.48, 8.13)	(6.75, 0)
	24.4±0.1	25.1±0.3	23.5±0.2	22.1±0.2	−1.7±0.1
100[c]	(22.97, 0)	(22.41, 8.13)	(15.88, 8.13)	(3.48, 8.13)	(6.47, 0)
	27.9±0.1	28.5±0.1	27.2±0.1	26.0±0.1	0.4±0.1
110[a]	(22.38, 0)	(22.41, 8.13)	(15.88, 8.13)	(3.48, 8.13)	(6.63, 0)
	24.6±0.2	25.5±0.1	23.8±0.1	22.3±0.1	−3.1±0.0
110[b]	(22.50, 0)	(22.41, 8.13)	(15.88, 8.13)	(3.48, 8.13)	(6.50, 0)
	23.0±0.2	23.9±0.1	22.1±0.1	20.4±0.1	−2.3±0.1
120[a]	(22.33, 0)	(22.41, 8.13)	(15.88, 8.13)	(3.48, 8.13)	(6.78, 0)
	24.4±0.1	25.4±0.1	23.6±0.1	22.1±0.1	−3.7±0.1
120[c]	(22.28, 0)	(22.41, 8.13)	(15.88, 8.13)	(3.48, 8.13)	(6.38, 0)
	26.6±0.0	27.4±0.2	25.7±0.1	24.6±0.1	−2.8±0.1
130[a]	(22.33, 0)	(22.41, 8.13)	(15.88, 8.13)	(3.48, 8.13)	(6.98, 0)
	25.0±0.0	26.1±0.0	24.1±0.1	22.4±0.1	−4.0±0.1
140[c]	(22.38, 0)	(22.41, 8.13)	(15.88, 8.13)	(3.48, 8.13)	(6.83, 0)
	27.2±0.1	28.2±0.2	26.4±0.1	25.2±0.1	−2.6±0.3
150[c]	(22.33, 0)	(22.41, 8.13)	(15.88, 8.13)	(3.48, 8.13)	(6.88, 0)
	26.4±0.2	27.4±0.1	25.6±0.1	24.4±0.1	−4.0±0.2
160[c]	(22.28, 0)	(22.41, 8.13)	(15.88, 8.13)	(3.48, 8.13)	(6.83, 0)
	27.1±0.1	28.1±0.1	26.2±0.1	24.9±02	−5.1±0.3

[a]The liquid temperature entering the evaporation chamber was 26 °C.
[b]The liquid temperature entering the evaporation chamber was 15 °C.
[c]The liquid temperature entering the evaporation chamber was 35 °C.

where A_I is the area of the liquid-vapor interface, the angle of the cone is ζ, the contact angle is denoted as θ (see Fig. 3), and the density of the liquid, the gravitational intensity, and the surface tension are denoted as ρ^L, g, and γ^{LV}. On the center line, the radii of curvature are equal and have the value R_c.

Also in Ref. [6] a numerical procedure is given for calculating A_I, θ, and R_c from the measured values of the width of the funnel at the position where the liquid-vapor interface intersects the funnel b, the measured value of ζ, and the measured height of the interface on the center line a. For all of the experiments, the value of b was 3.05 mm and ζ was 50°. For each of our experiments, the measured value of a is given in Table III along with the calculated value of the interfacial area A_I, R_c, and $\overline{Q}_V$.

B. Temperature profile in the liquid phase

Since we are not able to measure the mass flux at a point but only the average mass flux $\overline{j}$,

$$\overline{j} = \frac{1}{A_I} \int_{A_I} j \, dA, \tag{15}$$

it is necessary to use an approximate boundary condition to determine the temperature in the liquid phase. If the average heat flux from the liquid to the interface is denoted as $\overline{Q}_{IL}$, then it may be written in terms of the average mass flux and the average heat flux from the vapor to the interface

$$\overline{Q}_{IL} = \overline{j}(h^V - h^L) - \overline{Q}_V, \tag{16}$$

where h is the enthalpy.

To describe the liquid phase, we shall adopt spherical coordinates R^L, φ, ω. For the experiments that we consider the temperature of the water measured at the maximum depth in the glass funnel was less than 4 °C and still lower at the interface (see Table IV). In this temperature range, water expands with decreasing temperature; thus no buoyancy driven convection is expected. Also, we shall neglect forced

TABLE III. Interfacial properties and optimum values of Nu_B and $\overline{T}_{0B}$.

Liquid evaporation rate (μl/h)	Values of Nu_B and $\overline{T}_{0B}$	Height of interface at center a (mm)	Radius of interface at center R_c (mm)	Interface area (10^{-5}/m^2)	$\lvert\overline{Q}_V\rvert$ (W/m^2)
70[a]	9.26, −0.177	6.28	4.42	6.947	133.8±0.5
75[b]	9.41, −0.191	6.69	4.39	8.190	132.9±0.7
85[b]	9.39, −0.200	6.56	4.47	7.745	139.5±0.4
90[a]	9.12, −0.208	6.42	4.27	7.331	150.0±0.5
100[b]	9.41, −0.224	6.45	3.95	7.499	153.9±0.1
100[b]	9.28, −0.237	6.63	4.31	7.982	162.1±0.1
100[c]	9.15, −0.216	6.30	4.60	6.994	164.6±1.1
110[a]	9.14, −0.245	6.48	4.36	7.483	168.9±0.7
110[b]	9.56, −0.219	6.32	4.44	7.025	152.7±0.3
120[a]	9.15, −0.262	6.66	4.15	8.133	176.9±0.0
120[c]	9.07, −0.245	6.26	4.13	6.855	177.6±0.1
130[a]	9.22, −0.287	6.79	4.12	8.661	191.1±0.1
140[c]	8.95, −0.286	6.60	4.27	7.869	190.8±0.2
150[c]	8.90, −0.295	6.68	4.17	8.185	196.9±1.5
160[c]	9.00, −0.307	6.70	4.18	8.243	202.3±1.0

[a]The liquid temperature entering the evaporation chamber was 26 °C.
[b]The liquid temperature entering the evaporation chamber was 15 °C.
[c]The liquid temperature entering the evaporation chamber was 35 °C.

convective and gravitational effects and assume axial symmetry [6]. The liquid phase may be considered in two portions: one inside the cone and the other above the mouth of the cone (see Fig. 3). For the liquid within the cone, the heat flux through the walls of the funnel will be neglected since the funnel is in the double-walled evaporation chamber. Hence, within that portion of the liquid phase, the heat flux through any cross-sectional area would have the same value and be given by

$$Q_L = -\kappa^L \frac{T^L_{NI}}{a}\left(\frac{\partial \overline{T}^L}{\partial \overline{R}}\right),$$

where the temperature in the liquid phase has been nondimensionalized by T^L_{NI} and the radial coordinate by a. Then at position R^L the cross-sectional area is denoted as $A(R^L)$ and if Eq. (16) is applied one finds

TABLE IV. $\overline{Q}_{IL}$ and boundary condition temperatures measured in the liquid.

Liquid evaporation rate (μl/h)	$\overline{Q}_{IL}$ (W/m^2)	Position $[R^L_1$ (mm), 0] and measured temp T^L_1 (°C)	Position $[R^L_2$ (mm), 0] and measured temperature T^L_{NI} (°C)
70[a]	566.2±0.5	(3.90, 0)1.0±0.1	(6.10, 0)−0.2±0.1
75[b]	504.8±0.7	(3.78, 0)1.8±0.2	(6.48, 0)−2.8±0.1
85[b]	626.3±0.3	(3.93, 0)−3.6±0.1	(6.33, 0)−4.7±0.1
90[a]	706.8±0.5	(3.33, 0)−3.8±0.1	(6.23, 0)−5.1±0.0
100[b]	779.7±0.1	(3.23, 0)−7.1±0.1	(6.23, 0)−8.7±0.2
100[b]	714.2±0.2	(3.75, 0)−6.2±0.1	(6.55, 0)−7.6±0.1
100[c]	835.5±1.1	(3.97, 0)−6.2±0.0	(6.07, 0)−7.7±0.0
110[a]	861.7±0.7	(3.38, 0)−8.7±0.0	(6.18, 0)−10.5±0.0
110[b]	944.7±0.3	(4.0, 0)−9.0±0.0	(6.1, 0)−10.2±0.0
120[a]	858.0±0.3	(3.83, 0)−9.6±0.0	(6.53, 0)−11.0±0.2
120[c]	1049.7±0.1	(3.28, 0)−8.3±0.0	(6.08, 0)−10.5±0.1
130[a]	862.1±0.1	(4.33, 0)−10.6±0.1	(6.63, 0)−11.8±0.0
140[c]	1058.3±0.3	(4.38, 0)−11.1±0.1	(6.38, 0)−12.3±0.1
150[c]	1090.9±1.6	(3.83, 0)−11.7±0.0	(6.53, 0)−13.4±0.0
160[c]	1162.2±2.2	(4.78, 0)−13.2±0.2	(6.48, 0)−14.5±0.0

[a]The liquid temperature entering the evaporation chamber was 26 °C.
[b]The liquid temperature entering the evaporation chamber was 15 °C.
[c]The liquid temperature entering the evaporation chamber was 35 °C.

$$-\kappa^L \frac{T_{NI}^L}{a}\left(\frac{\partial \overline{T}}{\partial \overline{R}}\right)_{\overline{R}=\overline{R}_1} = \frac{A(R_1^L)}{A_I}[\overline{j}(h^V-h^L)-\overline{Q}_V]$$

$$(0 \leqslant \varphi \leqslant \varphi_{\max}). \quad (17)$$

Also the temperature in the liquid must equal to that measured on the center line at R_1 and R_2. Thus

$$\overline{T}(\overline{R}_2,0)=1 \quad (18)$$

and

$$\overline{T}(\overline{R}_1,0)=T_1^L/T_{NI}^L. \quad (19)$$

For each experiment, the measured temperatures T_{NI}^L and T_1^L, at the positions of R_2^L and R_1^L, and the value of $\overline{Q}_{IL}$ are listed in Table IV.

For the portion of the liquid that is above the mouth of the cone, the temperature depends on both R^L, φ and satisfies

$$\nabla^2 T=0. \quad (20)$$

By separation of variables, one finds that if the separation constant is denoted as t,

$$\overline{T}(\overline{R},\varphi)=\sum_{t=0}^{\infty}\left(D_t\overline{R}^t+\frac{G_t}{\overline{R}^{1+t}}\right)U_t(\cos\ \varphi), \quad (21)$$

where $U_t(\cos\varphi)$ is the Legendre polynomial. After differentiating with respect to $\overline{R}$, multiplying by a Legendre polynomial, and integrating the result

$$\left(tD_t\overline{R}^{t-1}-\frac{(1+t)G_t}{\overline{R}^{2+t}}\right)=\frac{2t+1}{2}\int_{\cos\varphi_{\max}}^{1}\left(\frac{\partial \overline{T}}{\partial \overline{R}}\right)U_t(x)dx. \quad (22)$$

It was found in Ref. [6] that the temperature in the liquid was described very well if Eq. (22) was approximated as

$$tD_t(\overline{R}_2)^{t-1}-\frac{(1+t)G_t}{(\overline{R}_2)^{2+t}} = -(2t+1)A(R_2^L)\frac{a\overline{Q}_{IL}}{2\kappa^L T_{NI}^L A_I}\int_{\cos\varphi_{\max}}^{1}U_t(x)dx. \quad (23)$$

This amounts to neglecting the φ dependence of

$$\left(\frac{\partial \overline{T}}{\partial \overline{R}}\right)_{\overline{R}=\overline{R}_2}. \quad (24)$$

This assumption is necessary since only the average flux is measured, but this assumption can be evaluated by comparing the predicted profile in the liquid with that measured.

After the boundary conditions given in Eqs. (17)–(19) and (23) are imposed, one finds the expression for the coefficients to be given by

$$D_0=\frac{\overline{R}_2-\sum_{t=1}^{\infty}\left(D_t(\overline{R}_2)^{t+1}+\frac{G_t}{(\overline{R}_2)^t}\right)}{\overline{R}_2-\overline{R}_1} - \frac{\overline{R}_1\left[\frac{T_1^L}{T_{NI}^L}-\sum_{t=1}^{\infty}\left(D_t(\overline{R}_2)^t+\frac{G_t}{(\overline{R}_2)^{t+1}}\right)\right]}{(\overline{R}_2-\overline{R}_1)}, \quad (25)$$

$$G_0=\overline{R}_2-\sum_{t=1}^{\infty}\left(D_t(\overline{R}_2)^{t+1}+\frac{G_t}{(\overline{R}_2)^t}\right)-(\overline{R}_2)D_0 \quad (26)$$

and for $t \geqslant 1$

$$D_t=\frac{(2t+1)}{t}\left(\frac{(\overline{R}_1)^{t+4}-(\overline{R}_2)^{t+4}}{(\overline{R}_2)^{2t+1}-(\overline{R}_1)^{2t+1}}\right)\Phi_t, \quad (27)$$

$$G_t=\left(\frac{t}{t+1}\right)(\overline{R}_2)^{2t+1}D_t+\left(\frac{2t+1}{t+1}\right)(\overline{R}_2)^{t+4}\Phi_t, \quad (28)$$

where

$$\Phi_t=\frac{\pi a^3\overline{Q}_{IL}}{\kappa^L T_{NI}^L A_I}(1-\cos\ \varphi_{\max})\int_{\cos\varphi_{\max}}^{1}U_t(x)dx. \quad (29)$$

Once Eqs. (25)–(28) are substituted into Eq. (21), one has the expression for the temperature in the liquid phase.

V. TEMPERATURE NEAR THE PHASE BOUNDARY

If the vapor is at a pressure P and the molecules are approximated as hard spheres of diameter d, then the expression for the mean free path (MFP) $P_{\rm MF}$ is [12]

$$P_{\rm MF}=\frac{kT}{\sqrt{2}\pi P d^2}, \quad (30)$$

where k is the Boltzmann constant. To estimate the molecular diameter, the relation between the viscosity $\mu_{\rm vap}$ and molecular size was used [13]:

$$d=\left\{\frac{1}{3\pi\mu_{\rm vap}}\sqrt{\frac{3mkT}{2}}\right\}^{1/2}, \quad (31)$$

where m is the mass of a molecule. The values of the MFP for each water experiment are listed in Table I. As may be seen there, the position closest to the interface where the temperature was measured was within a few MFPs of the interface. However, because of the analytical procedure developed in Sec. IV, it is the temperature measured at the position $(\hat{z},0)$ that is used to predict the temperature field. We first investigate the sensitivity of the calculated temperature field to the value chosen for $\hat{z}$.

In Fig. 6 the temperature calculated on the center line in both phases for the experiment with the highest rate of evaporation is shown. In Fig. 6(a) the temperature calculated based on the temperature measured with the thick thermocouple is shown. The value of $\hat{z}$ was chosen to be approxi-

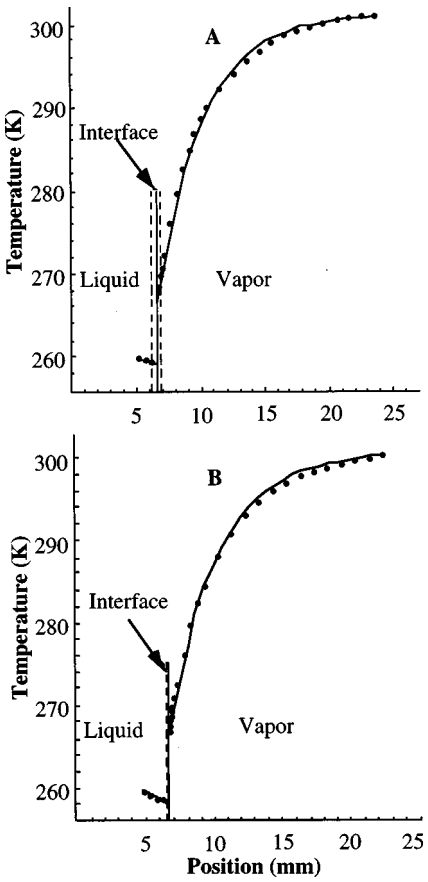

FIG. 6. Measured and calculated temperature profile when the liquid evaporation rate was 160 μl/h. The measurements are indicated by the solid dots and the calculations by the solid curved lines. The solid vertical line indicates the position of the interface and the dashed vertical lines indicate the position closest to the interface when a measurement was made. (a) Temperatures measured with a 81.3-μm-diam thermocouple. (b) Temperatures measured with a 25.4-μm-diam thermocouple.

mately seven MFPs from the interface and the value of the temperature measured there was -4.7 °C. Using this value of the temperature, the other boundary condition temperatures listed in Table II, and the analytical methods of Sec. IV, the temperature profile seen in Fig. 6(a) was obtained. As may be seen in this figure, there is little if any disagreement between the predicted and measured temperature on the center line. For this large thermocouple, it was not possible to measure the temperature closer than seven MFPs of the interface.

The results shown in Fig. 6(b) were obtained with the thinner thermocouple. In this case the value of $\hat{z}$ was chosen as approximately five MFPs from the interface and the temperature measured there was -5.1 °C. The temperature calculated on the center line using this value of the temperature and $\hat{z}$ along with the other boundary condition temperatures listed in Table II may be seen in Fig. 6(b), where it may be compared with the temperature measured at other positions on the center line. The agreement between the calculated and measured temperatures is equally as good as that obtained with the thicker thermocouple. As may be seen in Fig. 5, the temperatures measured by the two differently sized thermocouples are also in good agreement with one another. This

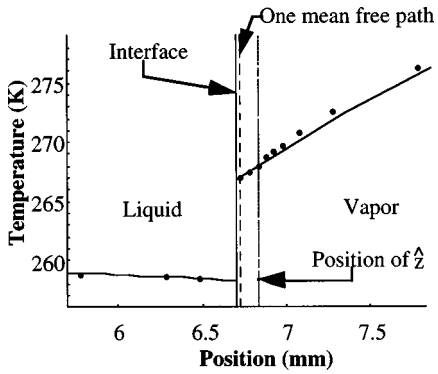

FIG. 7. Measured and calculated temperature profiles near the interface when the liquid evaporation rate was 160 μl/h. The measurements are made with the small thermocouple and indicated by the solid dots and the calculations by the solid curved lines. The solid vertical line indicates the position of the interface and the dashed vertical lines indicate the position of one mean free path. The dotted vertical line indicates the position of $\hat{z}$.

supports the claim of Ref. [6] that the temperature field calculated is insensitive to the value of $\hat{z}$ that is chosen.

Since the temperature in the vapor could be measured closer than five MFPs of the interface with the thinner thermocouple, we may assess the validity of the temperature calculated with the continuum energy equation within the Knudsen layer. We take this layer to be closer than five MFPs of the interface. In Fig. 7 an expanded view of the calculations and measurements near the interface is shown. As seen there, the temperatures that were measured within the Knudsen layer are in close agreement with the temperatures calculated from the continuum energy equation that were based on the temperature measured at five MFPs from the interface and the other boundary temperatures listed in Table II. There is no indication of a sudden decrease in the temperature either from the measurements or from the calculations. We would emphasize that the temperature calculated in this region does not represent an extrapolation since the polynomials used to calculate the temperature in the vapor spanned the vapor from the height of the cone mouth to the top of the vapor phase.

In the liquid phase, the procedure used to calculate the temperature leads to slightly better agreement with the measurements. The maximum difference between the measured and predicted temperatures in the liquid in our 15 experiments varied from 0.2 °C to 0.6 °C. When the temperature was calculated in the liquid phase at the interface, it was found to be less than that in the vapor in each of our experiments. The interfacial values obtained in each case are shown in Table V.

The temperature profile on the center line for the highest rate of evaporation experiment is shown in Fig. 5. The value of the MFP obtained from Eqs. (30) and (31) was 25.3 μm. This distance is equal to the diameter of the thin thermocouple wire and equal approximately to the radius of the thermocouple junction. Thus there would be on average no collisions of the molecules leaving the liquid before they encountered the thermocouple junction and an equal number of molecules from the vapor would be expected to encounter the junction. Hence, if there were a sudden temperature decrease within the Knudsen layer to a value that was less than

TABLE V. Calculated temperatures in liquid and vapor phases at the interface. TC denotes thermocouple.

Liquid evaporation rate (μl/h)	Temperature on the vapor side of the interface[a] ($\pm$deviation) (°C)	Temperature on the liquid side of the interface[a] ($\pm$deviation) (°C)	Maximum difference of measured and calculated temperature on the center line (°C)	Maximum difference of measured and calculated temperature on the chamber wall (°C)	Temperature difference across the interface by a 25-μm TC (°C)
70[b]	3.2±0.1	−0.3±0.1	0.9	0.7	3.5±0.2
75[c]	0.6±0.1	−2.9±0.1	0.7	0.6	3.5±0.2
85[c]	−0.6±0.1	−4.8±0.1	1.1	0.7	4.2±0.2
90[b]	−1.0±0.1	−5.2±0.0	0.9	0.7	4.2±0.1
100[c]	−3.8±0.1	−8.9±0.1	1.1	0.7	5.1±0.2
100[c]	−2.7±0.1	−7.7±0.2	0.6	1.0	5.0±0.3
100[d]	−1.6±0.2	−7.8±0.0	1.1	0.7	6.2±0.2
110[b]	−4.6±0.1	−10.7±0.1	0.9	0.7	6.1±0.2
110[c]	−4.3±0.2	−10.3±0.0	1.0	1.0	6.0±0.2
120[b]	−4.9±0.0	−11.0±0.2	0.9	0.8	6.1±0.2
120[d]	−4.1±0.1	−10.6±0.1	0.9	0.8	6.5±0.2
130[b]	−6.0±0.0	−11.9±0.1	0.9	1.0	5.9±0.1
140[d]	−5.2±0.1	−12.4±0.1	1.1	0.8	7.2±0.2
150[d]	−6.2±0.1	−13.5±0.0	1.1	0.7	7.3±0.1
160[d]	−6.8±0.4	−14.6±0.0	0.7	0.9	7.8±0.4

[a]Temperature calculated at the interface.
[b]The liquid temperature entering the evaporation chamber was 26 °C.
[c]The liquid temperature entering the evaporation chamber was 15 °C.
[d]The liquid temperature entering the evaporation chamber was 35 °C.

the temperature of the liquid, it should have been measured by the small thermocouple. As may be seen in Fig. 5(b), no such decease was observed.

The measurements indicate that the temperature in the vapor at the interface is greater than that in the liquid at the interface and that the difference between the temperatures increases with increasing rates of evaporation, reaching 7.8 °C. By contrast, the studies based on classical kinetic theory or nonequilibrium thermodynamics give as the expression for the temperature discontinuity [1,2,7]

$$T_i^V - T_i^L = (-0.45) M T_2^V \sqrt{\frac{\gamma}{2}}, \tag{32}$$

where M is the Mach number and γ is the ratio of specific heats. From Eq. (32) one finds that the predicted temperature discontinuity is 0.027 °C and in the opposite direction to that measured. Thus it seems that there is clearly disagreement between the predictions of classical kinetic theory or nonequilibrium thermodynamics with these measurements. The standard assumption in continuum mechanics is to assume that the temperatures at the interface in the two phases are equal. This ''intuitive'' assumption is also in disagreement with the measurements.

It seems appropriate to ask if there could be an error in the measurements. The values of the temperature listed in Table V were obtained with the temperature measured at $\hat{z}$ by the thin thermocouple. If the values of the temperature measured at $\hat{z}$ with the thick thermocouple are used to determine the temperature discontinuity, then one finds that the maximum difference in the values of temperature discontinuity obtained with the differently sized thermocouples is 0.6 °C. Thus the error in the measured values of the temperature discontinuity would be approximately this value. There is no evidence that heat conduction along the thermocouples significantly affected the measured value of the temperature.

In this series of experiments, compared with those of Ref. [6], the experimental apparatus was altered to allow the liquid to enter the evaporation chamber at different but controlled temperatures and to allow the pressure in the vapor phase to be significantly reduced. This permitted higher evaporation rates to be studied, strongly reduced the gradient of the temperature in the liquid phase, and increased the

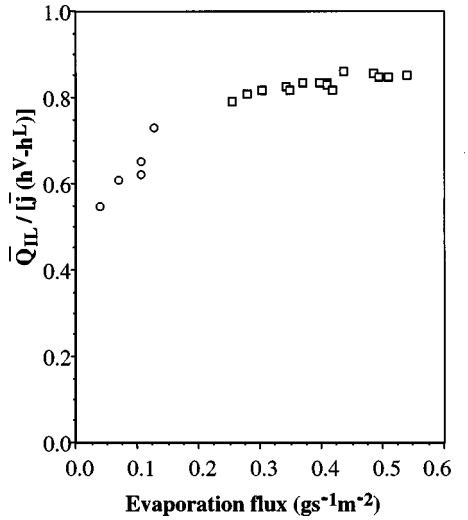

FIG. 8. Comparison of the nondimensional heat flux in the liquid phase between the experiments with the liquid inlet temperature control and experiments in which water entered at room temperature. The open square indicates the water experiments with temperature control and the open circle indicates the experiments in which water entered at room temperature.

MFP in the vapor. To determine if the experimental results obtained in this series of experiments are consistent with those of Ref. [6], the nondimensional variable

$$\frac{\overline{Q}_{IL}}{\overline{j}(h^V - h^L)} \tag{33}$$

from each series of experiments has been plotted for the different evaporation rates studied. The result is shown in Fig. 8; as seen there, the two sets of experimental results appear to be consistent with one another.

Since a thermocouple placed in the vapor approximately one MFP from the interface indicates that the temperature there is higher than that in the liquid at the interface by as much as 7.8 °C, it appears that the molecules ''escaping'' the liquid are on average the higher-energy molecules. At present there does not appear to be any explanation for this observation from classical mechanics. It remains to be seen if quantum mechanics will provide an explanation.

ACKNOWLEDGMENTS

This work was supported by the Natural Sciences and Engineering Research Council of Canada and the Canadian Space Agency.

[1] K. Aoki and C. Cercignani, Phys. Fluids **26**, 1163 (1983).
[2] Y.-P. Pao, Phys. Fluids **14**, 306 (1971); **16**, 1560(E) (1971); **16**, 1340 (1973); C. E. Siewert and J. R. Thomas, Jr., *ibid.* **16**, 1557 (1973); J. W. Cipolla, Jr., H. Lang, and S. K. Loyalka, J. Chem. Phys. **61**, 69 (1974).
[3] P. N. Shankar and M. D. Deshpande, Phys. Fluids A **2**, 1030 (1990).
[4] L. D. Koffman, M. S. Plesset, and L. Lees, Phys. Fluids **27**, 876 (1984).
[5] C. Cercignani, W. Fiszdon, and A. Frezzontti, Phys. Fluids **28**, 3237 (1985).
[6] C. A. Ward and G. Fang (unpublished).
[7] D. Bedeaux, L. J. F. Hermans, and T. Ytrehus, Physica A **169**, 263 (1990).
[8] C. Cercignani, *Theory and Application of the Boltzmann Equation* (Scottish Academic Press, Edinburgh, 1975), p. 127.
[9] M. H. Attia and L. Kops, J. Eng. Industry **110**, 7 (1988).
[10] J. Nanigian, Adv. Mater. Processes **12**, 66 (1994).
[11] A. K. Ray, J. Lee, and H. L. Tilley, Langmuir **4**, 631 (1988).
[12] R. D. Present, *Kinetic Theory of Gases* (McGraw-Hill, New York, 1958), p. 32.
[13] R. D. Present, Kinetic Theory of Gases (Ref. [12]), p. 44.